

## Observation of Two Time Scales in the Ferromagnetic Manganite $\text{La}_{1-x}\text{Ca}_x\text{MnO}_3$ , $x \approx 0.3$

R. H. Heffner,<sup>1</sup> J. E. Sonier,<sup>1</sup> D. E. MacLaughlin,<sup>2</sup> G. J. Nieuwenhuys,<sup>3</sup> G. Ehlers,<sup>4</sup> F. Mezei,<sup>1</sup> S.-W. Cheong,<sup>5</sup>  
J. S. Gardner,<sup>1</sup> and H. Röder<sup>1</sup>

<sup>1</sup>*Los Alamos National Laboratory, Los Alamos, New Mexico 87545*

<sup>2</sup>*Department of Physics, University of California, Riverside, California 92521*

<sup>3</sup>*Kamerlingh Onnes Laboratory, Leiden University, P.O. Box 9504, 2300 RA Leiden, The Netherlands*

<sup>4</sup>*Institute Laue Langevin, 38042 Grenoble Cedex 9, France*

<sup>5</sup>*Department of Physics and Astronomy, Rutgers University, Piscataway, New Jersey 08854*

(Received 23 August 1999)

We report new zero-field muon spin relaxation and neutron spin echo measurements in ferromagnetic (FM)  $(\text{La}, \text{Ca})\text{MnO}_3$  which suggest at least two spatially separated regions possessing very different Mn-ion spin dynamics. One region displays diffusive relaxation, “critical slowing down” near  $T_C$  and an increasing volume fraction below  $T_C$ , suggesting overdamped FM spin waves below  $T_C$ . The second region possesses more slowly fluctuating spins, a linewidth independent of  $q$ , and a decreasing volume fraction below  $T_C$ . The estimated length scale for the inhomogeneity is  $\leq 30$  Å.

PACS numbers: 75.30.Vn, 75.40.Gb, 76.75.+i, 78.70.Nx

It is clear that the richness in the temperature-composition phase diagram for  $\text{La}_{1-x}\text{Ca}_x\text{MnO}_3$  [1] is produced by a strong interplay between spin, charge, and lattice degrees of freedom [2]. Of particular interest has been the ferromagnetic (FM) insulator-to-metal transition and its accompanying large magnetoresistance. Millis and collaborators [3] first suggested that the theoretical description of this transition must include the electron-phonon Jahn-Teller (JT) coupling, in addition to the double-exchange [4] spin-spin interaction, thus invoking polaronic degrees of freedom. Experimental signatures of small-polaron hopping have emerged from transport measurements above the FM critical temperature  $T_C$  [5], leading to a theoretical description of magnetoelastic polarons in terms of a small cluster of aligned Mn spins surrounding a local JT lattice distortion [3,6].

Despite these important insights, an experimental and theoretical description of the FM transition encompassing *all three* important degrees of freedom (lattice, charge, and spin) remains incomplete. The persistence of two distinct local lattice distortions below  $T_C$  is clear from neutron pair-distribution function and x-ray absorption fine structure measurements [7,8]. A two-fluid model for the charge degrees of freedom is consistent with the evolution of localized charges into itinerant carriers near  $T_C$  [9]. However, a comparable description of the behavior of the spin system near  $T_C$  is lacking. Neutron scattering studies of the low-temperature magnetic properties [10] in FM perovskites have revealed a broad peak centered around zero energy transfer which coexists with Mn spin waves near  $T_C$  [11,12]. No definitive interpretation of this peak has emerged.

In this Letter we present new muon spin relaxation ( $\mu\text{SR}$ ) and neutron spin echo (NSE) measurements in FM  $\text{La}_{1-x}\text{Ca}_x\text{MnO}_3$ ,  $x \approx 0.3$ . NSE [13] allows a direct, high-resolution measurement of the spin-spin correlation

function  $S(q, t)$ . The muon is a local probe (bound within 1 Å of an O atom in oxide materials [14]) and is, therefore, sensitive to spatial inhomogeneity in spin fluctuation rates. Furthermore, the  $\mu\text{SR}$  technique [15] covers a wide range of correlation times ( $10^{-12} < \tau < 10^{-4}$  s), which overlaps that of NSE (typically  $10^{-11} < \tau < 10^{-9}$  s).

The  $\mu\text{SR}$  data were taken at the Paul Scherrer Institute in Villigen, Switzerland, and at TRIUMF in Vancouver, Canada, between 10 and 300 K. The NSE data were taken at 275 K with the IN11 spectrometer at the Institute Laue Langevin, using incident neutron wavelengths of 4 and 6 Å. All measurements were performed in zero applied field ( $\leq 1$  Oe) on polycrystalline samples. The  $\mu\text{SR}$  sample [ $x = 0.33$ ,  $T_C = 262(3)$  K from magnetization measurements] was from the same batch as that used in Ref. [16]. The NSE sample,  $x = 0.30$ , showed  $T_C = 250(5)$  K from magnetization measurements. This sample depolarized the neutron beam below about 270 K, indicating the onset of randomly oriented FM domains at a temperature somewhat above the nominal  $T_C$ . In general, polycrystalline materials of  $(\text{La}, \text{Ca})\text{MnO}_3$  possess less residual stress and are more compositionally homogeneous than comparable volumes of single crystals, because of relatively less Ca evaporation and more stable growth conditions.

The  $\mu\text{SR}$  data could be fit to a relaxation function  $G_z(t) = A_{\text{osc}}G_{\text{osc}}(t) + A_{\text{rlx}}G_{\text{rlx}}(t)$ , corresponding to oscillating and relaxing terms, respectively. The overall muon decay asymmetry was  $\approx 0.2$ ; here  $A_{\text{osc}} + A_{\text{rlx}} \equiv 1$ .  $G_{\text{osc}}(t)$  is given by  $A_{\text{osc}} \exp(-t/T_2) \cos(\omega_\mu t + \phi_\mu)$ , where  $1/T_2$  is the inhomogeneous damping rate, and  $\omega_\mu$  is the muon precession frequency. The frequency  $\omega_\mu(T)$  tends to zero at a temperature of 266(2) K, in agreement with  $T_C$  from magnetization measurements. We find that  $A_{\text{osc}} \approx 2/3$ , which for a polycrystal indicates that the entire sample volume experiences growth of the sublattice magnetization [16].

The relaxing component  $G_{\text{rlx}}(t)$  describes the local spin dynamics. In a typical magnetic material,  $G_{\text{rlx}}(t)$  is given by an exponential function  $A_{\text{rlx}} \exp(-\lambda t)$ , where  $\lambda = 1/T_1$  is the characteristic spin lattice relaxation rate [17,18]. In  $\text{La}_{0.67}\text{Ca}_{0.33}\text{MnO}_3$ , however, a single exponential function does not describe  $G_{\text{rlx}}(t)$  at temperatures below  $\approx 274$  K, as shown in Fig. 1(a). Earlier  $\mu\text{SR}$  data in  $\text{La}_{0.67}\text{Ca}_{0.33}\text{MnO}_3$  [16] were characterized with a stretched-exponential function,  $A_{\text{rlx}} \exp(-\lambda t)^K$ , where values of  $K < 1$  imply a distribution of rates  $\lambda$ . The current  $\mu\text{SR}$  data are of greater statistical precision than previously reported, and are taken at smaller temperature intervals near  $T_C$ , allowing observation of the rapid decline of  $K$  to about 0.2 just below  $T_C$ .

The simplest form to represent a distributed relaxation rate  $\Gamma$  is a bimodal distribution  $P(\Gamma) \propto A_1 \delta(\Gamma - \Gamma_1) + A_2 \delta(\Gamma - \Gamma_2)$ , corresponding to a two-exponential fit for either  $S(q, t)$  or  $G_{\text{rlx}}(t)$ . Figure 1(a) illustrates the nonexponential decay of  $G_{\text{rlx}}(t)$ . In Fig. 1(b) we plot  $G_{\text{rlx}}(t)$  in the form  $-t/\ln(G_{\text{rlx}})$ , together with the calculated curves from the fits to the stretched- and two-exponential functions shown in Fig. 1(a) [ $A_{\text{rlx}}$

is normalized to 1 in Fig. 1(b)]. Clearly, the two-exponential model function yields a considerably better representation of the data. Analysis at lower temperatures yields similar results.

For rapid fluctuations, the local muon relaxation rate  $\lambda$  is given by  $\lambda \propto \gamma_\mu^2 \sum_q |\delta B(q)|^2 \tau(q)$ , where  $|\delta B(q)|$  is the amplitude of the fluctuating local field and  $\tau(q)$  is the Mn-ion correlation time with wave number  $q$ . For the two-exponential function  $G_{\text{rlx}}(t) = A_f \exp(-\lambda_f t) + A_s \exp(-\lambda_s t)$ , with  $A_f + A_s = A_{\text{rlx}}$ , we have labeled the rates  $\lambda_f$  and  $\lambda_s$  to correspond to ‘‘fast’’ (short  $\tau$ ) and ‘‘slow’’ (long  $\tau$ ) Mn-ion fluctuation rates. Figure 2 shows the temperature dependence of the  $\mu\text{SR}$  parameters  $A_f$ ,  $A_s$ ,  $\lambda_f$ , and  $\lambda_s$ . For temperatures below 185 K and above about 270 K, either the overall relaxation rate is too small or the exponent  $K$  is too close to 1 to resolve two exponentials clearly. The peak value of  $\lambda_f$  coincides with  $\omega_\mu(T) \rightarrow 0$  at  $T \approx T_C$ . By contrast, the temperature dependence of  $\lambda_s$  shows no significant maximum near  $T_C$ , but rises slowly

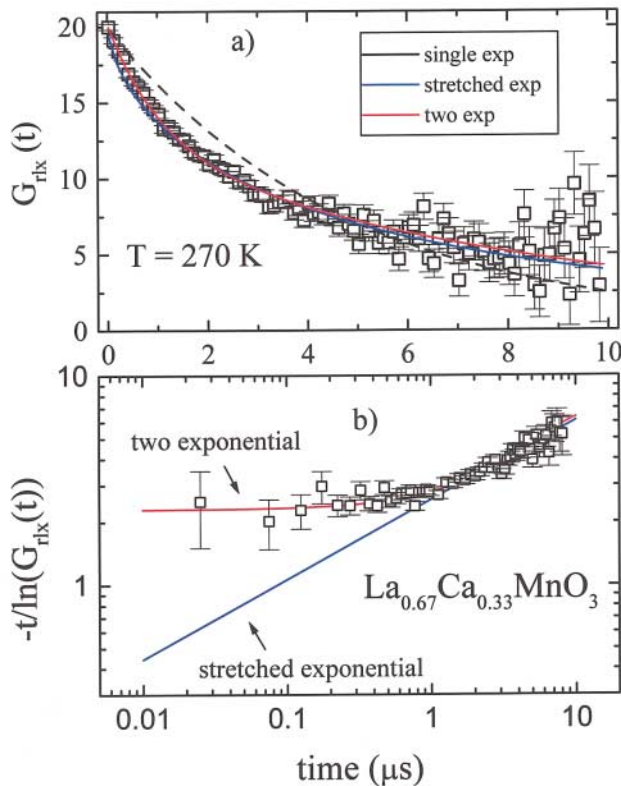


FIG. 1 (color). (a) Unnormalized  $\mu\text{SR}$  relaxation function  $G_{\text{rlx}}(t)$ . The lines show best fits using stretched exponential [ $\lambda = 0.219(7)$ ,  $K = 0.63(3)$ ], exponential [ $K = 1$ ], and two-exponential [ $A_f = 0.60(5)$ ,  $A_s = 0.40(5)$ ,  $\lambda_f = 0.106(5)$ , and  $\lambda_s = 0.93(11)$ ] functions defined in the text. (b) Same  $G_{\text{rlx}}(t)$  as in (a), normalized to  $G_{\text{rlx}}(0) = 1$ . The curves are the stretched and two-exponential fits of (a).

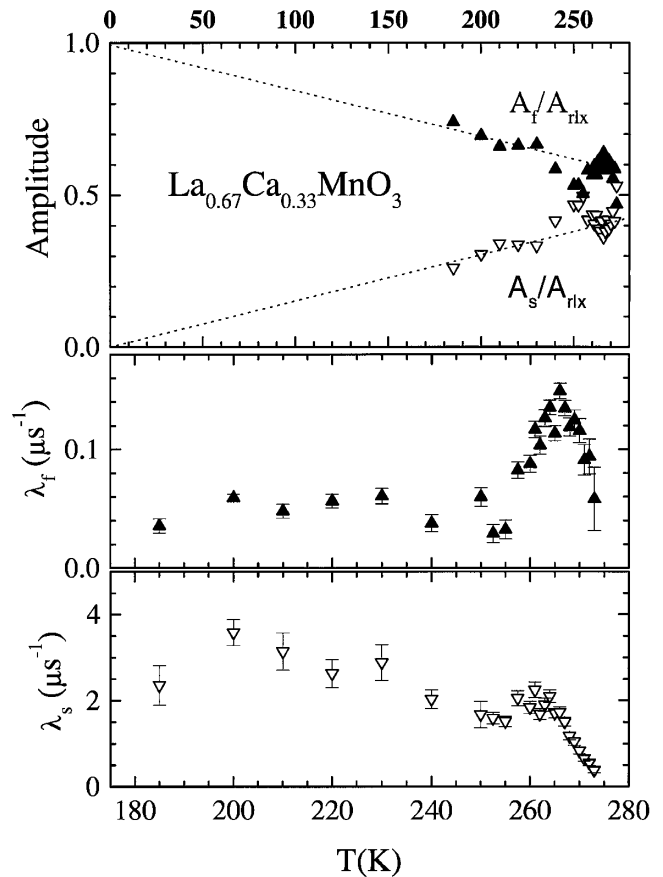


FIG. 2. Temperature dependence of  $\mu\text{SR}$  amplitudes  $A_f/A_{\text{rlx}}$  and  $A_s/A_{\text{rlx}}$  (top) and their respective relaxation rates  $\lambda_f$  (middle) and  $\lambda_s$  (bottom) for a two-exponential fit. The subscripts  $f$  (filled symbols) and  $s$  (open symbols) refer to fast and slow Mn relaxation rates  $\Gamma_{\text{Mn}}$ , respectively (see text, noting that  $\lambda \propto 1/\Gamma_{\text{Mn}}$ ). The dotted lines in the top frame show the trends extrapolated to  $T = 0$  K. Note the different temperature scales for the top and lower two frames.

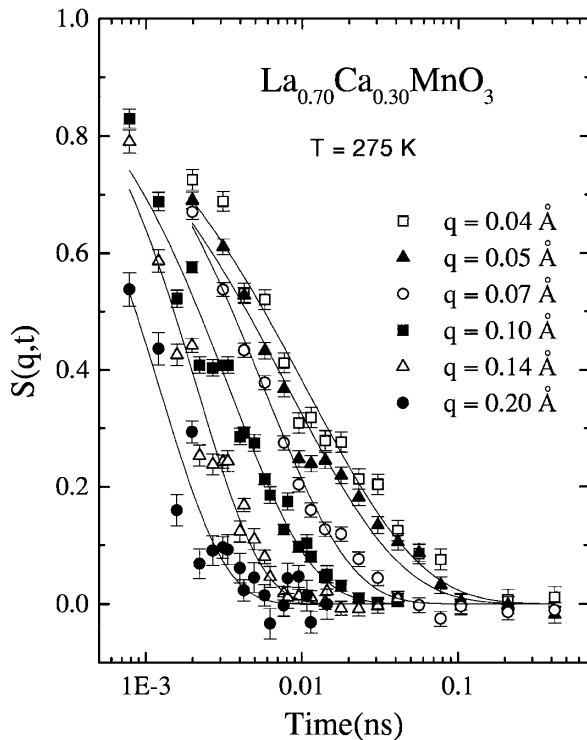


FIG. 3. NSE spin-spin correlation function  $S(q, t)$ . The data for  $q \geq 0.10 \text{ \AA}^{-1}$  were taken at incident wavelengths of 4 and 6  $\text{\AA}$  and, hence, extend to shorter times than data for  $q < 0.10 \text{ \AA}^{-1}$ , taken only at 6  $\text{\AA}$ .

below the critical temperature. The dotted lines (Fig. 2, top) are guides to the eye and indicate that the trend of  $A_f$  is to approach 100% of the fluctuating amplitude at  $T = 0 \text{ K}$ .

A distribution of  $\lambda$  implies that  $\delta B$  and/or  $\tau$  are distributed but does not determine the distributions separately, whereas  $S(q, t)$  gives a direct measure of the distribution of  $\tau(q)$  only. Figure 3 displays  $S(q, t)$  at  $T = 275 \text{ K}$  in  $\text{La}_{0.70}\text{Ca}_{0.30}\text{MnO}_3$ . The data can be fit either to  $S(q, t) = \exp[-(t/\tau_e)^\beta]$  or to  $S(q, t) = A_F \exp[-(t/\tau_F(q))] + A_S \exp[-(t/\tau_S(q))]$ ,  $S(q, 0) = 1$ , as shown by the solid curves in Fig. 3. The parameters are given in Table I. These results, together with the  $\mu\text{SR}$  data, directly confirm that the Mn-ion correlation times are distributed.

The NSE data give a further important clue to the origin of the relaxation processes. In Fig. 4, we plot

$\tau_F^{-1}$  and  $\tau_S^{-1}$  ( $0.04 \leq q \leq 0.10$ ) and  $\tau_e^{-1}$  ( $q = 0.14$  and  $0.20$ ) versus  $q^2$ . The data appear to fall on two parallel lines (rate  $\propto q^2$ ), one of which has a finite intercept at  $q = 0$ . A least squares fit to the upper line in Fig. 4 yields  $\tau_F^{-1} = Dq^2 + \Gamma_0$ , with  $D = 22(8) \text{ ps}^{-1} \text{ \AA}^2$  and  $\Gamma_0 = 0.20(3) \text{ ps}^{-1}$ . A fit to the lower line ( $\tau_S^{-1}$  and  $\tau_e^{-1}$ ) yields  $D = 21.1(5) \text{ ps}^{-1} \text{ \AA}^2$  and  $\Gamma_0 = -0.02(1) \text{ ps}^{-1}$ . Thus there are two time scales,  $\Gamma_1 = Dq^2$ , where  $D \approx 14 \text{ meV \AA}^2$ , and  $\Gamma_0 \approx 2 \times 10^{11} \text{ s}^{-1}$ .

An order of magnitude comparison to the measured  $\mu\text{SR}$  rates  $\lambda_f$  and  $\lambda_s$  can be made as follows. For rapid Mn fluctuation rates  $\Gamma_{\text{Mn}} \gg \omega_\mu$ , one has [15]  $\lambda = 2\omega_\mu^2/\Gamma_{\text{Mn}}$ . Here we ignore the  $q$  dependence of the muon-Mn coupling constant, which we take to be the value of the low-temperature  $\mu\text{SR}$  frequency  $\omega_\mu = 4.7 \times 10^8 \text{ rad/s}$  [16]. For  $\Gamma_{\text{Mn}} = \Gamma_0$ , one obtains  $\lambda \approx 2.2 \mu\text{s}^{-1}$ . For  $\Gamma_{\text{Mn}} = \Gamma_1$ , after a simple integration over  $q$ , one obtains  $\lambda \approx 0.01 \mu\text{s}^{-1}$ . These values (particularly their ratios) are in reasonable agreement with  $\lambda_s$  and  $\lambda_f$  at  $T \approx T_C$ . Thus we associate the  $q$ -independent Mn rate  $\Gamma_0$  with  $\lambda_s$  and the diffusive relaxation Mn rate  $\Gamma_1$  with  $\lambda_f$ .

These  $\mu\text{SR}$  and NSE data provide strong evidence for at least two spatially separated relaxation components near the FM state of  $(\text{La}, \text{Ca})\text{MnO}_3$ . This can be inferred from the  $\mu\text{SR}$  data alone because, although the  $\lambda_f$  component may exist throughout the sample volume, the  $\lambda_s$  component can exist only in spatially separated regions; otherwise only the slow Mn fluctuation rate (which creates the largest  $\mu\text{SR}$  rate) would be observed. Furthermore, we emphasize that, because of the large spin wave stiffness constant observed [11] near  $T_C$  in this material, the muon spin is not significantly relaxed via spin waves [16].

The diffusive component observed here with NSE has about the same diffusion constant  $D$  as that of the quasielastic ‘‘central peak’’ reported earlier by Lynn *et al.* [11], and is therefore likely the same excitation. The  $\mu\text{SR}$  rate  $\lambda_f$  tracks the temperature dependence of the linewidth associated with these fluctuations, showing a peak at  $T_C$ . These excitations thus appear to be FM excitations of limited spatial and temporal extent, becoming overdamped spin waves below  $T_C$ . Their diffusive relaxation could be caused by a lack of translational symmetry arising from disorder in the system. A rough estimate of the characteristic length scale for the underlying inhomogeneity (corresponding to a diffusive mean free

TABLE I. Fitting parameters for NSE spin-spin function  $S(q, t)$  in  $\text{La}_{0.70}\text{Ca}_{0.30}\text{MnO}_3$ ,  $T = 275 \text{ K}$ . Symbols are defined in the text.

$q$ ( $\text{\AA}^{-1}$ )	$\beta$	$\tau_e$ (ps)	$A_F$	$A_S$	$\tau_F$ (ps)	$\tau_S$ (ps)
0.04	0.59(4)	10.6(5)	0.63(5)	0.37(5)	4.2(6)	41(8)
0.05	0.60(4)	8.1(3)	0.70(4)	0.30(4)	4.0(4)	40(4)
0.07	0.78(6)	5.7(2)	0.67(9)	0.33(9)	3.5(5)	15(3)
0.10	0.82(4)	3.6(1)	0.55(21)	0.47(22)	1.8(6)	7(2)
0.14	1.06(7)	2.1(1)	...	...	...	...
0.20	1.03(9)	1.22(1)	...	...	...	...

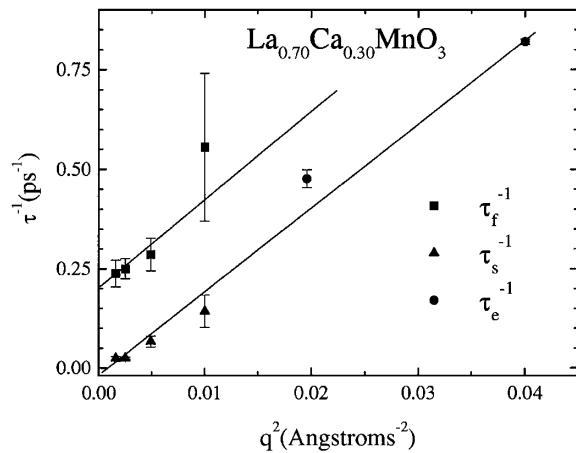


FIG. 4. NSE linewidths  $\tau_f^{-1}$ ,  $\tau_s^{-1}$ , and  $\tau_e^{-1}$  from Table I versus the square of the momentum transfer  $q^2$  at  $T = 275$  K. The solid lines are least squares fits to the form  $\tau^{-1} = \Gamma_1 + \Gamma_0$ , where  $\Gamma_1 = Dq^2$ .

path  $\bar{l}$ ) can be made. Noting that NSE probes excitations of wavelength  $\Lambda \approx 2\pi/q$  and that  $\bar{l} \leq \Lambda$  in order for  $\Gamma_1$  to follow a  $q^2$  dependence up to the largest measured  $q$  value ( $0.20 \text{ \AA}^{-1}$ ), we find that  $\bar{l} \leq 30 \text{ \AA}$ .

The lack of  $q$  dependence for  $\Gamma_0$  implies a local excitation. A fluctuation rate  $\approx 10^{-11} \text{ s}^{-1}$  is probably too slow to be associated with electronic relaxation of localized  $\text{Mn}^{3+}$  or  $\text{Mn}^{4+}$  spins. Polarons are localized objects, but the temperature dependence of the slow  $\mu\text{SR}$  rate  $\lambda_s$  does not show the typical exponentially activated behavior measured [5] for polaron hopping and associated with the conductivity of this system. Other possible mechanisms include phonon induced spin relaxation (via magnetoelastic coupling), two-level excitations or the slow overturning of spins associated with local polaron hopping in regions where spin and charge motion are frustrated by more extreme local lattice distortions; that is, regions which are relatively *insulating*. The latter possibility is qualitatively consistent with the temperature dependence of  $\lambda_s$ , which increases slowly below  $T_C$ , and of the volume fraction  $A_s$ , which decreases below  $T_C$  as the material becomes more and more metallic. Nevertheless, we are unable to definitively identify the cause of the  $\lambda_s$  ( $\Gamma_0$ ) relaxation.

In conclusion, there are at least three types of fluctuations below  $T_C$  in FM  $\text{La}_{1-x}\text{Ca}_x\text{MnO}_3$ . In addition to FM spin waves reported elsewhere [10,11], there is a localized mode of unknown origin and a diffusive component probably associated with overdamped spin waves below  $T_C$ . We emphasize that the  $\mu\text{SR}$  data show that the spin lattice relaxation must be *spatially* inhomogeneous. This spatial distribution of spin fluctuation rates is probably related to the disordered spatial distribution of La and Ca ions and the corresponding fluctuations in the local lat-

tice distortions. (Persistence of structural inhomogeneity considerably below  $T_C$  has been found by local probes of the lattice structure [7,8,19], which are consistent with the *gradual* loss of structural inhomogeneity below  $T_C$ .) A rough estimate of the characteristic length scale of the inhomogeneity  $\bar{l} \leq 30 \text{ \AA}$ . These data thus point to the need for explicitly including fine scale spatial and temporal inhomogeneity when modeling the spin degrees of freedom in the manganites.

Work at Los Alamos was performed under the auspices of the U.S. DOE. Work elsewhere was supported in part by the U.S. NSF, Grant No. DMR-9731361 (University of California, Riverside), and by the Dutch Foundations FOM and NWO (Leiden).

- [1] Sang-Wook Cheong and Harold Y. Hwang, in "Colossal Magnetoresistance Oxides," edited by Y. Tokura (Gordon and Breach, New York, to be published).
- [2] *The Physics of Manganites*, edited by T.A. Kaplan and S.D. Mahanti (Kluwer Academic/Plenum, New York, 1999); Colossal Magnetoresistance Oxides, Ref. [1] (to be published).
- [3] A. J. Millis *et al.*, Phys. Rev. Lett. **74**, 5144 (1995); Phys. Rev. B **54**, 5389 (1996); **54**, 5405 (1996).
- [4] C. Zener, Phys. Rev. **82**, 403 (1951); P. W. Anderson and H. Hasegawa, Phys. Rev. **100**, 675 (1955); P. G. DeGennes, Phys. Rev. **118**, 141 (1960).
- [5] M. F. Hundley *et al.*, Appl. Phys. Lett. **67**, 860 (1995); M. Jaime *et al.*, Phys. Rev. Lett. **78**, 951 (1997).
- [6] H. Röder *et al.*, Phys. Rev. Lett. **76**, 1356 (1996).
- [7] D. Louca *et al.*, Phys. Rev. B **56**, R8475 (1997); S. Billinge *et al.*, Phys. Rev. Lett. **77**, 715 (1996).
- [8] C. H. Booth *et al.*, Phys. Rev. Lett. **80**, 853 (1998); A. Lanzara *et al.*, Phys. Rev. Lett. **81**, 878 (1998).
- [9] M. Jaime *et al.*, Phys. Rev. B **60**, 1028 (1999).
- [10] J. A. Fernandez-Baca *et al.*, Phys. Rev. Lett. **80**, 4012 (1998); H. Y. Hwang *et al.*, Phys. Rev. Lett. **80**, 1316 (1998); T. G. Perring *et al.*, Phys. Rev. Lett. **77**, 711 (1996).
- [11] J. W. Lynn *et al.*, Phys. Rev. Lett. **76**, 4046 (1996); L. Vasiliu-Doloc *et al.*, J. Appl. Phys. **81**, 5491 (1997).
- [12] Some  $\text{La}_{0.67}\text{Ca}_{0.33}\text{MnO}_3$  samples do not show a "central peak," however. [See J. J. Rhyne *et al.*, J. Appl. Phys. **87**, 5813 (2000).] In light of our results, and those of Lynn *et al.* [11], this situation deserves further investigation.
- [13] *Neutron Spin Echo*, edited by F. Mezei (Springer-Verlag, Heidelberg, 1980); F. Mezei, Z. Phys. **255**, 146 (1972).
- [14] E. Holzschuh *et al.*, Phys. Rev. B **27**, 5294 (1983).
- [15] A. Schenck, *Muon Spin Rotation Spectroscopy: Principles and Applications to Solid State Physics* (Hilger, Bristol, 1985).
- [16] R. H. Heffner *et al.*, Phys. Rev. Lett. **77**, 1869 (1996).
- [17] T. Moriya, Prog. Theor. Phys. **28**, 371 (1962).
- [18] P. C. M. Gubbens *et al.*, Hyperfine Interact. **85**, 239 (1994).
- [19] S. J. L. Billinge *et al.*, Phys. Rev. B **62**, 1203 (2000).